Journal of Alloys and Compounds 501 (2010) 259–264

Contents lists available at ScienceDirect

Journal of Alloys and Compounds

journal homepage: www.elsevier.com/locate/jallcom

Effects of multi-doping of rare-earth oxides on the microstructure and dielectric properties of $BaTiO_3$

Soo Kyong Jo[a], Jae Sung Park[b], Young Ho Han[a,*]

[a] Department of Materials Engineering, Sungkyunkwan University, Suwon 440-746, Republic of Korea
[b] Samsung Electro-Mechanics Co., Suwon, Republic of Korea

ARTICLE INFO

Article history:
Received 23 October 2009
Received in revised form 12 April 2010
Accepted 15 April 2010
Available online 22 April 2010

Keywords:
Coating materials
Ferroelectrics
Chemical synthesis
Dielectric response
Oxide material
Microstructure

ABSTRACT

Effects of multi-doping of rare-earth oxides (R = Yb, Sm, Ho, La and Nd) on the microstructure development and electric properties of $BaTiO_3$ ceramics were studied. The addition of samarium oxide leads to poor densification and small grains, whereas ytterbium oxide develops large grains and secondary phases along the grain boundary, and Ho ion with an intermediate ionic radius gives rise to higher densities with fine grains. The grain size of Yb-doped $BaTiO_3$ decreased with increasing Sm contents. The system coated with 2.0 at.% Sm and 2.0 at.% Yb exhibited dense microstructures with uniform small grains, and Yb-rich second phases were not observed. It was confirmed that an appropriate ratio of donor to acceptor is necessary to the optimum microstructure. Curie temperature of rare-earth doped $BaTiO_3$ was strongly dependent on the unit-cell volume associated with the ionic sizes of rare-earth ions.

1. Introduction

Multilayer ceramic capacitor (MLCC) is one of the most important passive components in electronic devices such as hand held products, personal computer and digital display [1,2]. The development trend of MLCC is a miniaturization with increasing the capacitance. In order to achieve further downsizing or higher capacitances, the dielectric layers as well as electrode layers need to be reduced and nano-size particles with narrow size distribution should be prepared [1–4]. Currently, oxide additives are mechanically mixed with $BaTiO_3$ powders. However, it is difficult to achieve a homogeneous mixing between fine $BaTiO_3$ powders and various additives through the conventional ceramic process. As an alternative, the uniform coating of $BaTiO_3$ particles with a thin and stable additive oxide layer is the most promising approach for enhancing the homogeneous distribution of additives along the grain boundaries [5,6].

The chemical coating on ceramic powders has been attempted to investigate the doping effects and the surface characteristics of particles through various coating processes [5–12]. Chemical coating can produce a very homogeneous additives shell, regardless of particle size. A uniform coating of inorganic shells on the inorganic cores was reported to be caused by surface reaction [5]. Bassano et al. studied nano-coatings of several oxides (Y_2O_3, Dy_2O_3, ZrO_2, NiO) and reported a precipitation processes to grow a second-phase layer on the surface of $BaTiO_3$ particles [8]. Additives coating on $BaTiO_3$ powders have been carried out for X7R temperature characteristics, revealing the performance on the dielectric properties and microstructure [10]. The effects of additives coating on the powder characteristics, dielectric properties, and sintering behavior of $BaTiO_3$ system were also studied [11,12].

Rare-earth oxides such as Ho_2O_3, Er_2O_3 and Dy_2O_3 are important additives in the fabrication of $BaTiO_3$-based MLCC. They are frequently added to control the temperature coefficient of capacitance (TCC), grain growth, insulating electrical resistance and reliability [1,13–16]. Since the ionic radii of trivalent rare-earths (R^{3+}) range from 0.80 Å to 1.30 Å, these dopants could occupy either Ba^{2+} (1.61 Å) or Ti^{4+} (0.61 Å) sites, depending on the ionic radius and Ba/Ti ratio [14,17]. The microstructure development and electrical properties are strongly dependent on the site preference of rare-earth impurity in $BaTiO_3$ sublattices [13–16]. As the ionic radius increases, the behavior is increasingly donor-type, suggesting an increasing fractional occupation of Ba sites. For the larger ions such as Sm^{3+} and Nd^{3+}, the donor behavior is more pronounced in the samples with an excess of TiO_2. The cations of intermediate size seem to occupy both Ba and Ti sites to varying degrees, depending on their radii [16]. In the presence of excess TiO_2 it behaves as a weak donor, while in the presence of excess BaO it acts as an acceptor. Apparently it can be pushed from one site to the other depending on the Ba/Ti ratio. Electrical profiles of Yb-doped $BaTiO_3$

---

* Corresponding author. Tel.: +82 31 290 7392; fax: +82 31 290 7410.
E-mail address: yhhan@skku.ac.kr (Y.H. Han).

0925-8388/$ – see front matter © 2010 Elsevier B.V. All rights reserved.
doi:10.1016/j.jallcom.2010.04.085

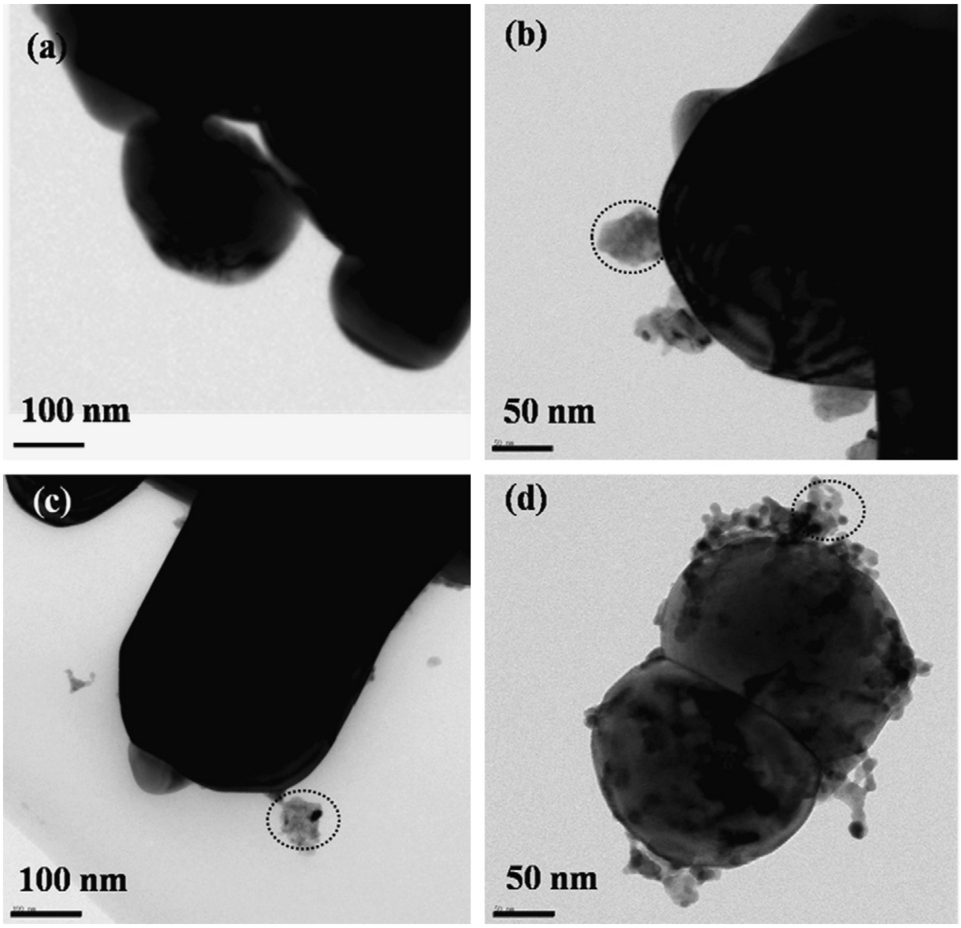

Fig. 1. TEM images of the coated particles: (a) $BaTiO_3$ powder as received, (b) Sm-coated $BaTiO_3$ powder, (c) Ho-coated $BaTiO_3$ powder and (d) Yb-coated $BaTiO_3$ powder.

show acceptor-type behavior with substitution on Ti site, regardless of the Ba/Ti ratio [16].

Numerous works have been conducted to confirm the singly-doping effects of rare-earth oxides on the microstructure and electrical properties of $BaTiO_3$-based systems [13–16,18]. However, few works were reported with regard to the electrical properties and microstructures of $BaTiO_3$ doped with two kinds of rare-earth oxides. In this study, the microstructure development and dielectric properties of $BaTiO_3$ doped with various combinations of trivalent rare-earth impurities have been investigated through the precipitation coating technique.

2. Experimental procedure

$BaTiO_3$ (Sakai, 300 nm) powders were coated with rare-earth oxides, which were prepared by a homogeneous precipitation method using reagent grade Samarium (III) Chloride Hexahydrate (>99.99%, $SmCl_3{\cdot}6H_2O$, Aldrich), Holmium (III) Chloride Hexahydrate (>99.99%, $HoCl_3{\cdot}6H_2O$, Aldrich), Ytterbium (III) Chloride Hexahydrate (99.99%, $YbCl_3{\cdot}6H_2O$, Aldrich) and urea (NH_2CONH_2, Aldrich). All solutions and suspensions were prepared in aqueous solution. $BaTiO_3$ (5 g) powders were dispersed in 100 ml of distilled water with continuous ultrasonic treatment (40 kHz) for 30 min to obtain a well-dispersed $BaTiO_3$ suspension. And additive solutions were added to the suspension with 1 M urea and dispersant. The molar ratio of $[R^{3+}]/[BaTiO_3]$ (R = Sm, Ho, Yb) were 0.01 and 0.02, where rare-earth oxides were 1 mol% and 2 mol%, respectively. The mixture was sonicated in a water bath and heated to 80 °C for 2 h in a thermostatic under stirring. The suspension was then aged in an electric oven at 90 °C for 12 h and calcination was conducted at 700 °C [5,11]. The powders were pulverized into fine particles and formed into a disk shape under a uniaxial pressure of 200 MPa. The organic binder was burned out at 450 °C in air with a slow heating rate, followed by sintering at 1350 °C for 2 h in air. Powder morphology and thermally etched surfaces of sintered specimens were investigated using a field emission scanning electron microscope (FESEM, Jeol-JSM7000F) and transmission electron microscopy (TEM, Jeol-300 kV) with an energy-dispersive spectroscope. The lattice parameter was obtained using an automated X-ray diffractometer (Bruker AXS D8 Discover) with Cu-Kα radiation. As a reference phase, α-Al_2O_3 was used to compensate the systematic error in the observation of 2θ values. The dielectric constant was measured over a temperature range from −55 °C to 151 °C using a capacitance measurement system (Saunders & Associate) with an LCR meter (HP4284A).

3. Results and discussion

Fig. 1 shows TEM images of $BaTiO_3$ particles coated with various rare-earth oxides (Sm, Ho, Yb). The precipitated samples were followed by calcination at 700 °C. The surface of $BaTiO_3$ particles as received looks smooth (Fig. 1a), whereas nano-size particles formed on the surfaces of $BaTiO_3$ and aggregated together instead of formation of a smooth film. EDS analysis confirmed that the heavily coated area was composed of rare-earth rich phases. This coating substance on $BaTiO_3$ is formed by the decomposition of urea and the reaction between $BaTiO_3$ and additive precursors. Urea is hydrolyzed according to the following reaction [5]:

$$(NH_2)_2CO + 3H_2O \rightarrow CO_2 + 2NH_3 + 2H_2O \quad (1)$$

By heating the solution, urea is decomposed into ammonia and carbon dioxide. Ammonium ions gradually increase pH of the solution and induce the precipitation of metal hydroxides [5]. The mixed precursors of samarium, holmium and ytterbium hydroxide would precipitate through the hydrolysis reaction of urea, the uniform precipitations of additive precursors in the presence of $BaTiO_3$ particles leading to the hetero-coagulation which produces homogeneous distribution of additives on the $BaTiO_3$ surface. It was

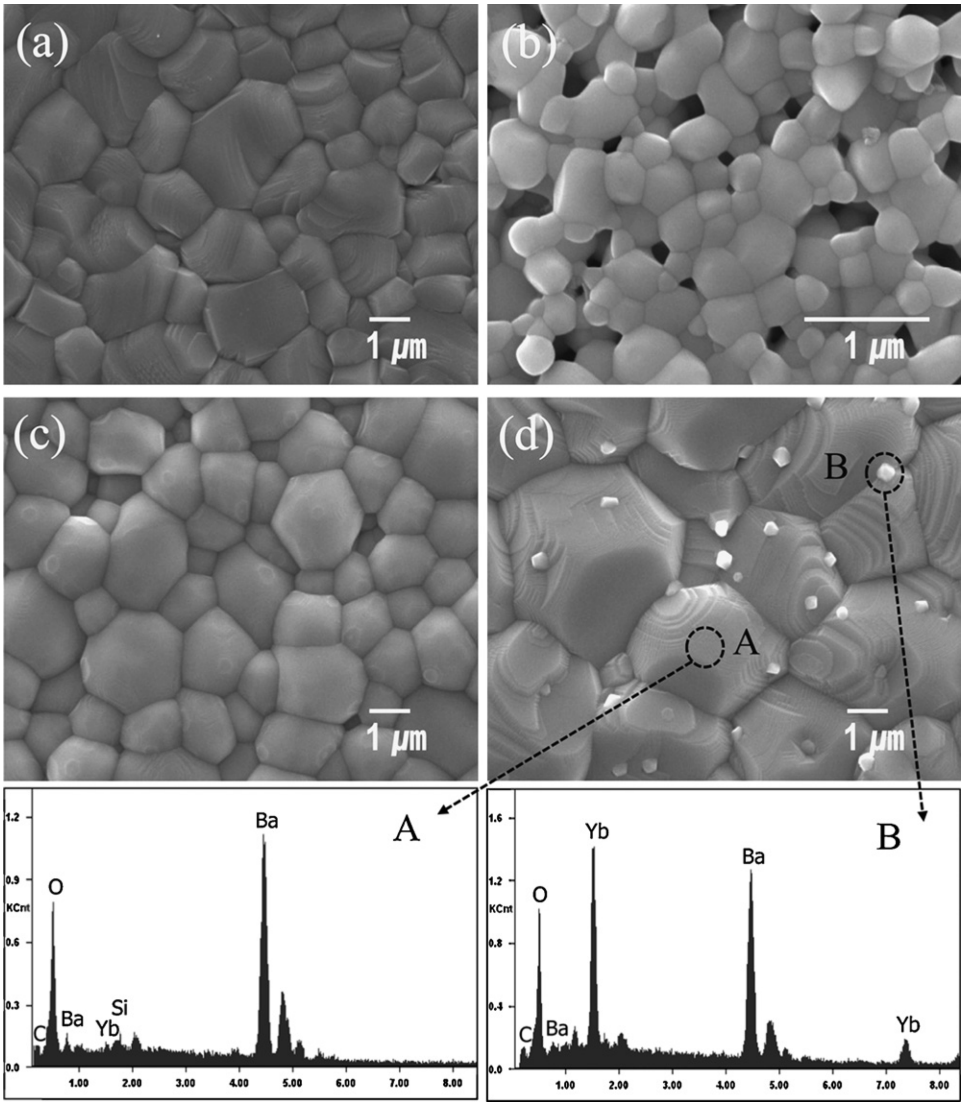

Fig. 2. Microstructures of rare-earth oxide coated $BaTiO_3$ sintered at 1350 °C: (a) un-doped $BaTiO_3$, (b) 2 at.% Sm coating, (c) 2 at.% Ho coating and (d) 2 at.% Yb coating.

reported that the hetero-coagulation behavior is dependent on the relative particle size, concentration of particles and surface charge [5,6].

Microstructures of un-doped and 2 at.% rare-earth coated $BaTiO_3$ specimens are shown in Fig. 2. The Sm-doped specimen shows poor densification and small grains, whereas the Yb-doped one exhibits large grains with a secondary phase along the grain boundary. It should be noted that Ho-doped specimen shows relatively high density with uniform grains, which looks similar to that of the un-doped $BaTiO_3$ (Fig. 2a). This could be due to the amphoteric behavior of Ho, holmium ions occupying both Ba and Ti sites, depending on the Ba/Ti ratio. Yb-doped specimen shows some segregation of second phase in the grain boundary and triple points, indicating that Yb hardly incorporates into the $BaTiO_3$ lattice. EDS results clearly exhibit the precipitation along the grain boundary comprising Yb-rich phases (Fig. 2d). This result is in good agreement with the previous work that the solubility of Yb ions must be lower than Sm and Ho ions [15].

Fig. 3 shows the microstructure of $BaTiO_3$ specimens co-doped with Sm ($\leq$2.0 at.%) and Yb (2.0 at.%) at various Sm/Yb ratios. The second phase was present with the Yb excess systems (Sm/Yb < 1) and gradually disappeared as the Sm content was increased, and none of the second phase was observed on the specimen co-doped with 2 at.% Sm and 2 at.% Yb (Fig. 3d). The grain size also decreased with increasing Sm additions to the Yb-coated $BaTiO_3$ systems. The system co-doped with Sm and Yb exhibits smaller grain sizes than the singly Yb-doped $BaTiO_3$, where Sm and Yb replace Ba and Ti sites, respectively, leading to a self-compensating substitution. The uniform and small grains of co-doped $BaTiO_3$ are compatible with the amphoteric behavior of Ho ions (Fig. 2c), where a half of Ho ions would equally split into Ba and Ti sites [14]. This result suggests that an appropriate ratio of donor/acceptor addition is necessary to the optimum microstructure development.

X-ray diffraction patterns of $BaTiO_3$ co-doped with Sm and Yb are given in Fig. 4. The secondary phase of $Ba_2Yb_2O_5$ was observed for singly Yb-doped $BaTiO_3$. The intensity of $Ba_2Yb_2O_5$ peaks decreased with increasing Sm contents. A weak trace of $Ba_2Yb_2O_5$ phase was detected with 2 at.% Sm and 2 at.% Yb co-doped $BaTiO_3$, compared with the singly Yb-doped samples. This implies that the main compensation mode is changed from Ba vacancies (V''_{Ba}) to Sm on Ba sites ($Sm^{\bullet}_{Ba}$) upon enhancing the Sm concentration at a constant Yb content. This is compatible with the evolution of microstructures shown in Fig. 3. The small ionic radius of Yb and its subsequent lower degree of incorporation into $BaTiO_3$ could be responsible for dielectric properties as well as microstructures.

Fig. 5 shows the dielectric constants for Sm, Ho, Yb and Yb–Sm-doped $BaTiO_3$ over the temperature range from −55 °C to 151 °C.

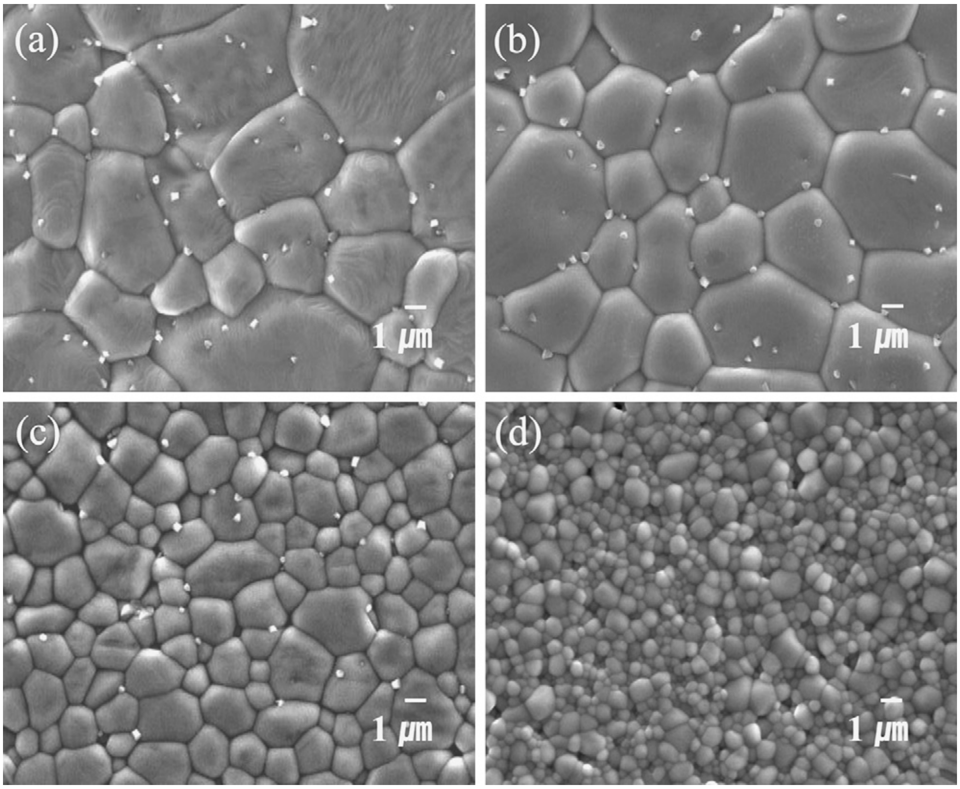

Fig. 3. Microstructures of Sm and Yb co-doed $BaTiO_3$ sintered at 1350 °C: (a) 2 at.% Yb, (b) 0.5 at.% Sm, 2 at.% Yb, (c) 1 at.% Sm, 2 at.% Yb and (d) 2 at.% Sm, 2 at.% Yb coating.

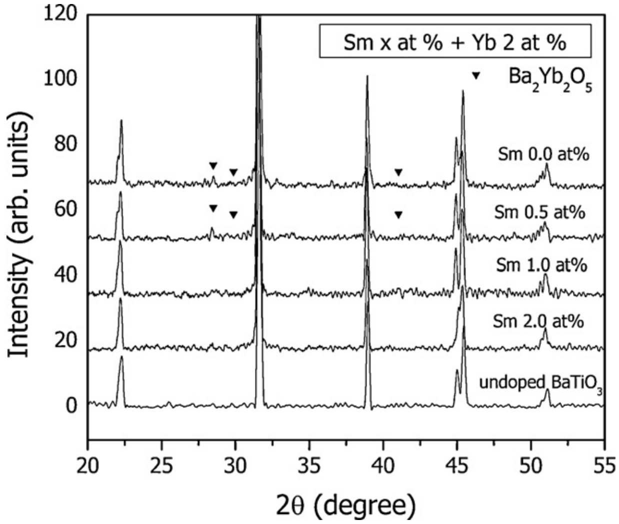

Fig. 4. X-ray diffraction patterns of $BaTiO_3$ co-doped with Sm and Yb.

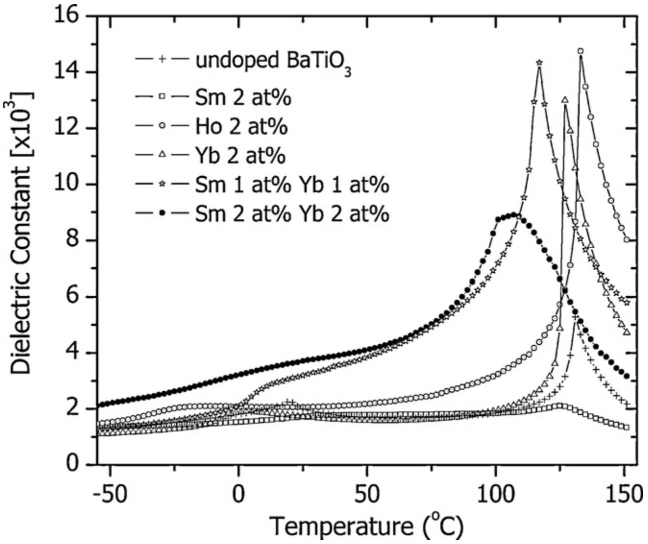

Fig. 5. Temperature dependence of dielectric constant of rare-earth doped and un-doped $BaTiO_3$.

The specimen co-doped with Sm and Yb shows higher dielectric values at room temperature and a significant depression of T_c, comparing with singly-rare-earth doped $BaTiO_3$. When the Sm content is greater than 0.5 mol%, the substitution of Sm^{3+} for Ba^{2+} ($Sm_{Ba}^{\bullet}$) would be compensated by cation vacancies instead of electron compensation as follows [13,16]:

$$Sm_2O_3 + 3TiO_2 \rightarrow 2Sm_{Ba}^{\bullet} + V_{Ba}'' + 3Ti_{Ti} + 9O_O \quad (2)$$

The defect notation is that suggested by Kröger and Vink [19]. V_{Ba}'' is the barium vacancy. The cation vacancies could inhibit grain growth [16]. The flat dielectric curve and low dielectric permittivity of Sm-doped specimen is thus due to the poor densification (Fig. 2b). The slight decrease in T_c could be due to the decrease in unit-cell volume by the substitution of smaller Sm^{3+} ion for larger Ba^{2+} ion [2,16]. Unlike the Sm-doped $BaTiO_3$ sample, the Ho-doped sample shows a subtle difference in T_c compared with the un-doped one. This result shows that Ho^{3+} ions could be split equally into both cation sites, giving rise to the self-compensation, as in the case of Er-doped $BaTiO_3$ ceramics [13,14]. The decrease in Curie point of the Yb-doped sample is due to the occupation of Yb^{3+} ion on Ti^{4+} sites as an acceptor impurity, Yb_{Ti}', and its compensating oxygen vacancy as follows:

$$2BaO + Yb_2O_3 \rightarrow 2Ba_{Ba} + 2Yb_{Ti}' + 5O_O + V_O^{\bullet\bullet} \quad (3)$$

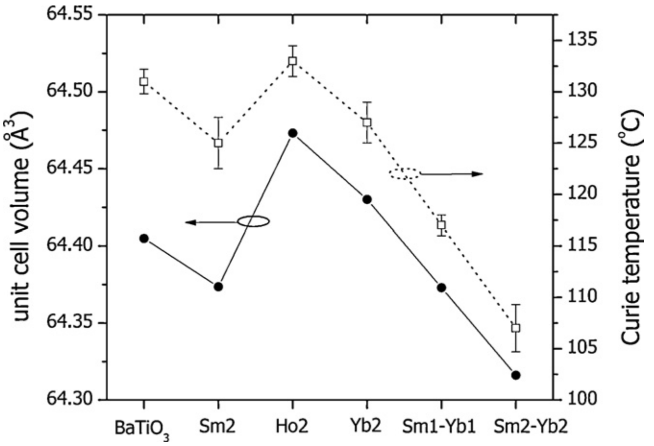

Fig. 6. The unit-cell volume and Curie temperature of various rare-earth doped and un-doped $BaTiO_3$, the number after each element stands for the added at.%.

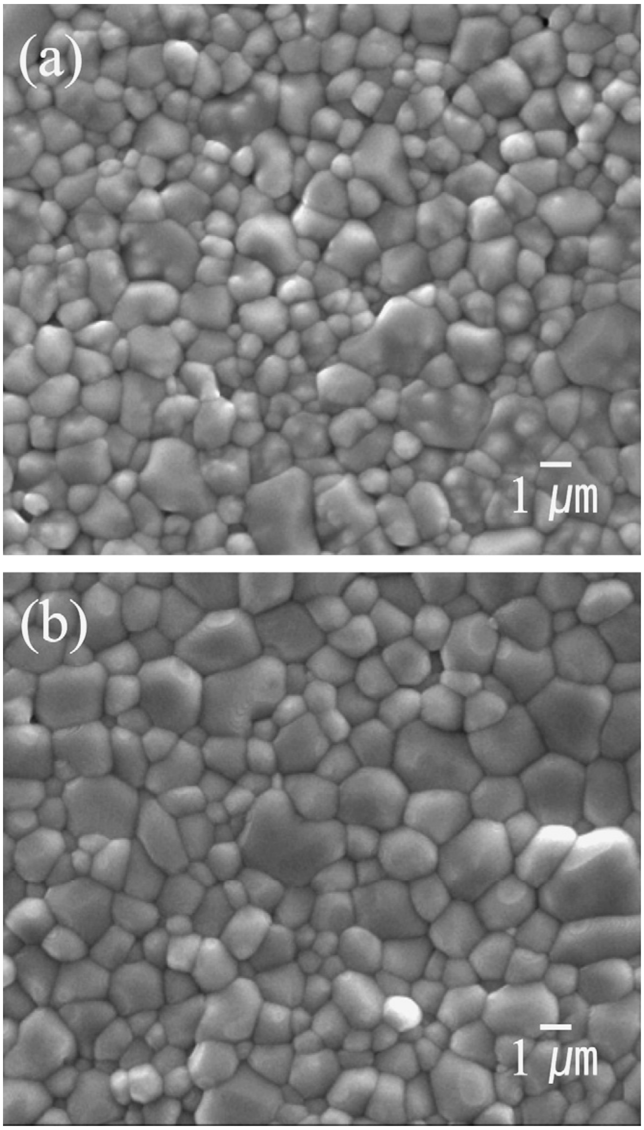

Fig. 7. Microstructures of rare-earth oxides co-doped $BaTiO_3$ sintered at 1350 °C: (a) 2 at.% Nd, 2 at.% Yb and (b) 2 at.% La, 2 at.% Yb.

In this case, the solubility of Yb in Ti sites is limiting. The Yb-rich second phase was observed in the grain boundary (Fig. 2d). However, the solubility seems enhanced in the presence of Sm as shown in Fig. 3d. The simultaneous substitution of Sm and Yb for Ba and Ti sites could increase the solubility of Yb, which could shift T_c to lower temperatures.

Fig. 6 shows unit-cell volumes and Curie temperatures of $BaTiO_3$ doped with various rare-earth ions. The unit-cell volumes and Curie temperatures exhibit a similar dependence on the doping materials [20]. The Sm-doped $BaTiO_3$ has a smaller unit-cell volume than the Ho-doped one, and the latter consequently has higher T_c than the former. This result supports that Ho ions have the amphoteric behavior and Sm ions occupy only Ba sites. The unit-cell volume and Curie point linearly decreased with increasing rare-earth oxide (Sm + Yb) contents. This result indicates that Sm and Yb ions obviously occupy Ba and Ti sites, respectively. It was thus confirmed that the unit-cell volume is dependent on the incorporation mode of the substituted ions as well as their ionic radii.

Fig. 7 shows the microstructures of $BaTiO_3$ specimens co-doped with Nd–Yb or La–Yb. Larger rare-earth ions such as Nd and La would obviously occupy Ba sites and enhance Yb to occupy Ti sites. The sintered specimens show uniform microstructures without any secondary phase such as $Ba_2Yb_2O_5$, which is similar to the microstructure shown in the Sm–Yb-doped system in Fig. 3d. The evolution of microstructure seems correlated with the combination of large and small dopant ions. A possible incorporation mode of large rare-earth ions (R_2O_3) with excess Yb_2O_3 into $BaTiO_3$ lattices can be written as follows:

$$R_2O_3 + Yb_2O_3 \rightarrow 2R^{\bullet}_{Ba} + 2Yb'_{Ti} + 6O_O (R = La, Nd, Sm) \qquad (4)$$

Eq. (4) shows that La, Nd and Sm ions with large ionic radii may replace Ba sites, whereas Yb ion with small ionic radius may occupy Ti sites and then gives rise to self-compensation, i.e. donor–acceptor compensation [16]. Thus, the $BaTiO_3$ system co-doped with large ions (La, Nd, Sm) and small ions (Yb) can effectively increase the solubility limit of rare-earth ions in $BaTiO_3$ and develop homogeneous microstructures.

4. Conclusions

The rare-earth coating on $BaTiO_3$ was performed by decomposition of urea and surface reaction between $BaTiO_3$ and additive (Sm, Ho, Yb) precursor. Samarium oxide leads to a poor densification with small grains, whereas ytterbium oxide develops large grains and secondary phase along the grain boundary. Holmium oxide with an intermediate ionic radius gives rise to high densification with fine grains. This could be due to the amphoteric behavior of Ho ions, occupying both Ba and Ti sites, depending on the Ba/Ti ratio. The grain size of singly Yb-doped $BaTiO_3$ decreased with increasing Sm contents. The specimen doped with 2.0 at.% Sm and 2.0 at.% Yb exhibits homogeneous microstructure without any Yb-rich second phase. It was confirmed that an appropriate ratio of donor to acceptor is necessary to the optimum microstructure development. Curie temperature of rare-earth doped $BaTiO_3$ was strongly dependent on the unit-cell volume which is associated with the ionic sizes of rare-earth ions and their incorporation modes into $BaTiO_3$ sublattices.

Acknowledgement

This research was supported by a grant from the Center for Advanced Materials Processing (CAMP) of the 21st Century Frontier R&D Program funded by the Ministry of Knowledge Economy (MKE), Republic of Korea. This research was also supported by the

Center for Ceramic Passive Components (CCPC) funded by Samsung Electro-Mechanics.

References

[1] H. Kishi, Y. Mizuno, H. Chazono, Base-metal electrode-multilayer ceramic capacitors: past, present and future perspectives, Jpn. J. Appl. Phys. 42 (2003) 1–15.

[2] Y. Sakabe, T. Reynolds, Base-metal electrode capacitors, Am. Ceram. Soc. Bull. 81 (2002) 24–26.

[3] D.F.K. Henning, Dielectric materials for sintering in reducing atmospheres, J. Eur. Ceram. Soc. 21 (2001) 1637–1642.

[4] A.J. Moulson, J.M. Herbert, Electroceramics Materials, Properties, Applications, second ed., John Wiley & Sons, 2003.

[5] E. Matijević, S.V. Babu, Colloid aspects of chemical–mechanical planarization, J. Colloid Interface Sci. 320 (2008) 219–237.

[6] F. Caruso, Nanoengineering of particle surfaces, Adv. Mater. 13 (2001) 11–22.

[7] F.A. Selmi, V.R.W. Amarakoon, Sol–gel coating of powders for processing electronic ceramics, J. Am. Ceram. Soc. 71 (1988) 934–937.

[8] A. Bassano, V. Buscaglia, M. Sennour, M.T. Buscaglia, M. Viviani, P. Nanni, Nanocrystalline oxide (Y_2O_3, Dy_2O_3, ZrO_2, NiO) coatings on $BaTiO_3$ submicron particles by precipitation, J. Nanopart. Res. (2009) (Published online 18 April).

[9] S.A. Bruno, D.K. Swanson, I. Burn, High-performance multilayer capacitor dielectrics from chemically prepared powders, J. Am. Ceram. Soc. 76 (1993) 1233–1241.

[10] S.F. Wang, G.O. Dayton, Dielectric properties of fine-grained barium titanate based X7R materials, J. Am. Ceram. Soc. 82 (1999) 2677–2682.

[11] J.S. Park, Y.H. Han, Effects of oxide additives coating on microstructure and dielectric properties of $BaTiO_3$, J. Electroceram. 17 (2006) 867–873.

[12] J.S. Park, Y.H. Han, Effects of MgO coating on microstructure and dielectric properties of $BaTiO_3$, J. Eur. Ceram. Soc. 27 (2007) 1077–1082.

[13] J.H. Hwang, Y.H. Han, Dielectric properties of erbium doped barium titanate, Jpn. J. Appl. Phys. 40 (2001) 676–679.

[14] Y. Tsur, T.D. Dunbar, C.A. Randall, Crystal and defect chemistry of rare earth cations in $BaTiO_3$, J. Electroceram. 7 (2001) 25–34.

[15] Y. Sakabe, Y. Hamaji, H. Sano, N. Wada, Effects of rare-earth oxides on the reliability of X7R dielectrics, Jpn. J. Appl. Phys. 41 (2002) 5668–5678.

[16] D.M. Smyth, The Defect Chemistry of Metal Oxides, Oxford, New York, 2000.

[17] R.D. Shannon, Revised effective ionic radii and systematic studies of interatomic distances in halides and chalcogenides, Acta Cryst. A32 (1976) 751–767.

[18] S.H. Yoon, J.H. Lee, D.Y. Kim, N.M. Hwang, Core–shell structure of acceptor-rich, coarse barium titanate grains, J. Am. Ceram. Soc. 85 (2002) 3111–3113.

[19] F.A. Kroger, H.J. Vink, Relation between the Concentrations of Imperfections in Crystalline Solids, in: Solid State Physics, Advances in Research and Applications, 3, 1956, pp. 307–435.

[20] B. Jaffe, W.R. Cook, H. Jaffe, Piezoelectric Ceramics, Academic Press, London, 1971.